Heliyon 10 (2024) e23119

Contents lists available at ScienceDirect

Heliyon

journal homepage: www.cell.com/heliyon

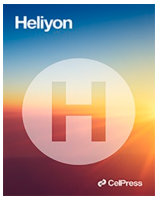

A novel ERβ high throughput microscopy platform for testing endocrine disrupting chemicals

Derek A. Abbott [a], Maureen G. Mancini [a,b], Michael J. Bolt [b,c], Adam T. Szafran [a,b], Kaley A. Neugebauer [d], Fabio Stossi [a,b,*], Daniel A. Gorelick [a,d], Michael A. Mancini [a,b,c,e,**]

[a] Department of Molecular and Cellular Biology, Baylor College of Medicine, Houston, TX, USA
[b] GCC Center for Advanced Microscopy and Image Informatics, Houston, TX, USA
[c] Center for Translational Cancer Research, Institute of Biosciences & Technology, Texas A&M University, Houston, TX, USA
[d] Center for Precision Environmental Health, Baylor College of Medicine, Houston, TX, USA
[e] Department of Pharmacology and Chemical Biology, Baylor College of Medicine, Houston, TX, USA

ARTICLE INFO

Keywords:
Estrogen receptor beta
High content analysis
High throughput microscopy
Endocrine disruptors
Zebrafish
Estrogen receptor alpha

ABSTRACT

In this study we present an inducible biosensor model for the Estrogen Receptor Beta (ERβ), GFP-ERβ:PRL-HeLa, a single-cell-based high throughput (HT) *in vitro* assay that allows direct visualization and measurement of GFP-tagged ERβ binding to ER-specific DNA response elements (EREs), ERβ-induced chromatin remodeling, and monitor transcriptional alterations via mRNA fluorescence in situ hybridization for a prolactin (PRL)-dsRED2 reporter gene. The model was used to accurately (Z' = 0.58–0.8) differentiate ERβ-selective ligands from ERα ligands when treated with a panel of selective agonists and antagonists. Next, we tested an Environmental Protection Agency (EPA)-provided set of 45 estrogenic reference chemicals with known ERα *in vivo* activity and identified several that activated ERβ as well, with varying sensitivity, including a subset that is completely novel. We then used an orthogonal ERE-containing transgenic zebrafish (ZF) model to cross validate ERβ and ERα selective activities at the organism level. Using this environmentally relevant ZF assay, some compounds were confirmed to have ERβ activity, validating the GFP-ERβ:PRL-HeLa assay as a screening tool for potential ERβ active endocrine disruptors (EDCs). These data demonstrate the value of sensitive multiplex mechanistic data gathered by the GFP-ERβ:PRL-HeLa assay coupled with an orthogonal zebrafish model to rapidly identify environmentally relevant ERβ EDCs and improve upon currently available screening tools for this understudied nuclear receptor.

1. Introduction

Estrogen Receptor-β (ERβ) is one of two ER steroid receptor subtypes (ERα and ERβ) that are targeted by the endogenous hormone,

* Corresponding author. GCC Center for Advanced Microscopy and Image Informatics, Department of Molecular and Cellular Biology, 117A Cullen Building, Baylor College of Medicine One Baylor Plaza Houston, TX 77030, USA.
** Corresponding author. GCC Center for Advanced Microscopy and Image Informatics Departments of Molecular and Cellular Biology, and Pharmacology and Chemical Biology 119A Cullen Building Baylor College of Medicine One Baylor Plaza Houston, TX 77030, 713, USA.
E-mail addresses: stossi@bcm.edu (F. Stossi), mancini@bcm.edu (M.A. Mancini).

https://doi.org/10.1016/j.heliyon.2023.e23119
Received 16 June 2023; Received in revised form 24 November 2023; Accepted 27 November 2023
Available online 8 December 2023

17β estradiol (E2). Both ERβ and ERα are ligand-activated transcription factors with ERβ being primarily expressed in prostate, bladder, colon, ovary, adipose tissues, and others [1,2]. Overall, although less studied as a target of environmental toxicants and drugs, ERβ is known to bind several phytoestrogens with potential clinical applications [3–6]. The two ER subtypes mechanistically work very similarly [1,5,7,8], requiring receptor dimerization after ligand binding, interaction with responsive DNA elements (Estrogen Response Elements - EREs) and recruitment of coregulators to modify transcriptional output. At the structural level, the two receptors display high homology in the DNA binding domain, subtle differences in the ligand binding domain, and very different N-terminal A/B domain [9,10]. Development of subtype-specific compounds has been a challenge due to the similarity of the ligand binding pockets. While ERα and ERβ share only 59 % total amino acid identity, the hormone binding pocket itself features only 2 amino acid changes; however, the ERα pocket is larger by ~100 Å, allowing compounds to be synthesized as ERα selective [9,11] based on the size of side chains. Despite this challenge, several natural and synthetic ERβ potency-selective compounds have been identified, including genistein, liquiritigenin, diarylpropionitrile (DPN), 4-[2-phenyl-5,7-bis(trifluoromethyl)pyrazolo[1,5-*a*]pyrimidin-3-yl]phenol (PHTTP), and others [3–5].

Developing high content, high throughput models of nuclear receptor activity has been of great interest over the past decades to aid in the evaluation of ligands, environmental perturbagens, and small molecule inhibitors, and to minimize reliance on expensive and time-consuming animal models. As the ERs are central in reproductive endocrinology, metabolism, immune responses and several diseases, the identification of molecules that would perturb the ER system, either in a positive or negative manner, has been paramount to characterize new potential drug treatments and to flag natural or man-made chemicals as effectors of this central cellular pathway [12,13].

It is now well accepted that hundreds, if not thousands, of chemicals and their mixtures greatly affect the ecosystem, including their role(s) in human pathophysiology [14–16]. Many of these chemicals have been introduced to the environment from pesticides, industrial waste, pharmaceuticals, etc. and have been shown to interfere with natural ER hormone responses. In general, such chemicals are labeled as endocrine disrupting chemicals (EDCs). Epidemiological studies have linked some EDCs to a range of pathophysiological conditions including cancer, metabolic and developmental defects [17–20]. Due to human health concerns from EDCs exposure, the Environmental Protection Agency (EPA) and the National Institute of Environmental Health Sciences (NIEHS) have started large programs (ToxCast and Tox21, for example, [21,22]) to generate and validate rapid and efficient high throughput assays and identify chemical compounds affecting ER and other nuclear receptor pathways. Toward this goal, a panel of 18 high throughput (HT) *in vitro* assays that report on different mechanistic features of ER were evaluated over thousands of chemical and, ultimately, a set of 45 compounds (EPA45) with known *in vivo* ERα activities (agonists, antagonists, and inactive controls) was utilized to create a mathematical model that was able to predict the estrogenic potential of a chemical *in vivo* [23,24]. Collectively, these HT assays focused on ERα, which is where the most studies on EDCs has been over the years, leading to a paucity of information about the effect of EDCs on ERβ, despite many phytoestrogens showing preferential ERβ activity [25–27].

During the past ~15 years, we have contributed to the field by creating a novel, high throughput, high content platform based upon a prolactin (PRL) promoter/enhancer model, linked to a reporter gene (dsRED2), that allows for fast and sensitive multiparametric analysis of the ER pathway. This platform, through visualization of a GFP-tagged ER bound to the PRL reporter gene locus (referred to as the chromosomal PRL 'array'), and allows measuring several steps of the ER pathway, notably EREs binding, coregulator recruitment, chromatin remodeling and transcriptional output all in one imaging-based, single cell endpoint assay, greatly enhancing content at high speed without losing throughput [28–33]. It is worth mentioning that the original ERα PRL array model was indeed included in the ToxCast 18 assays [21], albeit only in the context of GFP-ER binding the PRL locus. Using the same platform, we generated several additional biosensor cell lines for ERα [32], ERβ [29], Androgen Receptor [34], and Progesterone Receptor [35], all of which proved their power in describing small molecule and EDCs activities, from individual compounds to complex mixtures, that can also be used in case of environmental emergencies due to the fast response measurable by this assay (*i.e.,* 30 min of treatments followed by imaging).

In the original, stable, non-inducible ERβ PRL array model [29], we tested a small set of less-studied bisphenol A (BPA) analogs (BPXs) that identified how several BPXs bound ERβ and altered its activity, often in an antagonistic fashion. Compared to ERα, there is a scarcity of cell- and imaging-based contextual ERβ high throughput assays with only a non-nuclear-targeting, ligand binding domain-only assay (bimolecular fluorescence complementation assay - BiFC) being present in the ToxCast library [23].

Here, we describe the development and characterization of a second generation doxycycline-inducible GFP-ERβ:PRL-HeLa cell line. We show the selection of mechanistic features available within the assay, and assay accuracy and reproducibility features when challenged with compounds selective to ERα or ERβ. We tested the activity of the EPA45 reference compound set on ERβ and compared the results to published ERα datasets [32]. The results show that indeed our new model is sensitive to estrogenic compounds and identified many members of the EPA45 library as ERβ ligands. The addition of an orthogonal *in vivo* assay, a transgenic ERE-reporter zebrafish [36,37] validated some of the hits from the EPA45 library, further highlighting the importance of orthogonal assays to control for false positives/false negatives to address the effects of ligands on ERβ vs. ERα.

Together, these data demonstrate GFP-ERβ:PRL-HeLa as a robust assay filling an important void in our ability to characterize EDC activity on ERβ, potentially elucidating novel drug moieties, and environmental EDCs.

2. Materials and methods

2.1. Development of the tetracycline-inducible GFP-ERβ:PRL-HeLa cell line

The generation of the original PRL-HeLa cell model was described in detail previously [31]. In brief, the PRL model consist of HeLa

cell line containing a multi-integration of ~100 copies of an engineered transcriptional reporter unit consisting of the prolactin gene promoter linked, at the 3′ end, to a multimerized prolactin, ERE-rich, enhancer, and at the 5' end to a dsRED2 reporter gene. It is important to mention that HeLa cells do not express either estrogen receptor. PRL-HeLa cells expressing tetracycline (tet)-inducible full length (isoform 1) GFP-tagged ERβ were generated by first cloning the pEGFP-C1-ERβ (N-terminally tagged) coding region into pENTR shuttle vector using TOPO cloning. It is then transferred to pINDUCer20 using "Gateway" cloning, which includes a tetracycline-inducible promoter, a gift from Dr. Trey Westbrook (Baylor College of Medicine, Houston, TX). High titer packaged lentivirus was produced by System Biosciences LLC (Palo Alto, CA). PRL-HeLa cells were transduced with inducible GFP-ERβ viral particles and cells with a stable integration were enriched using Geneticin (G418) drug selection, flow cytometry, and single cell cloning. Selected clones were further validated with Western blotting and RNA FISH against the dsRED2 reporter gene.

2.2. Cell culture

The tet-inducible GFP-ERα:PRL-HeLa [32] and GFP-ERβ:PRL-HeLa cell lines were grown in phenol red-free Dulbecco's Modified Eagle's Medium (DMEM) containing 5 % tetracycline-free fetal bovine serum (FBS; Gemini Bioproducts), L-glutamine, 200 μg/ml hygromycin and 400 μg/ml G418. Before experimental treatments, cells were plated in DMEM containing 5 % charcoal dextran stripped and dialyzed FBS (SD-FBS) for 24 h before addition of 1 μg/ml amount of doxycycline for an additional 24 h. Note that SD-FBS is not assayed for tetracycline, however, little to no expression of GFP-ER was noted without addition of doxycycline dox treatment.

2.3. Chemicals, treatments, and screening setup

Every experiment included negative (dimethylsulfoxide, DMSO, 0.5 %) and positive controls (17β-estradiol, E2, 10 nM, (Sigma); 4-hydroxytamoxifen, 4HT, 100 nM (Sigma)). Information on additional chemicals can be found in Supplementary Table 1. The EPA45 library [23] was provided by Dr. Richard Judson (EPA) in pre-formatted, multi-well plates in DMSO at a known stock concentration. *In vitro* screening of the EPA45 library in GFP-ERβ:PRL-HeLa cells was performed at concentrations ranging from 0.1 pM to 100 μM (depending on the compound) and a treatment time of 2-h. EPA stock chemical solutions were transferred to template plates using a Biomek NX^P robot (Beckman Coulter). Working dilutions of compounds were then added in quadruplicate to assay plates containing prepared cells (Aurora Microplates 384 well plates, cells seeded at 2250 cells/well).

For zebrafish experiments, the chemicals were spotted in 96 well plates (PerkinElmer CellCarrier™ – 96 ultra) at a volume equal to 1/1000th of the total final volume/well. This was performed robotically using a Labcyte Echo 550 acoustic liquid handler at the Texas A&M Institute of Bioscience and Technology.

2.4. Immunofluorescence

Cells were fixed in 4 % EM-grade formaldehyde in PBS buffer (80 mM potassium PIPES [pH 6.8], 5 mM EGTA, and 2 mM $MgCl_2$) and quenched with 0.1 M ammonium chloride for 10 min. For samples in which no antibodies are used, cell membranes were permeabilized using 0.5 % Triton X-100 for 10 min and DNA stained using DAPI (1 μg/ml) for 10 min. For samples with antibody labeling, permeabilization was with 0.5 % Triton X-100 for 30 min. Cells were incubated at room temperature in blotto (5 % milk in Tris-buffered saline/Tween 20) for 30 min, and then primary antibodies (listed in Supplementary Table 2) were added overnight at 4 °C prior to 1 h of secondary antibody (AlexaFluor 647 conjugates; Molecular Probes, 1:1000) and DAPI staining (1 μg/ml for 10 min).

2.5. Single molecule RNA FISH (smFISH)

Cells were plated in a 384-well plate (2.25×10^3 cells/well, Aurora Microplates), and, after treatment, were fixed in EM-grade 4 % paraformaldehyde in RNAse-free phosphate-buffered saline for 20 min on ice and then permeabilized with 70 % ethanol in RNAse-free water at 4C overnight. Cells were washed in "wash buffer" (WB, 2X SSC and 10 % formamide) followed by hybridization in "hybridization buffer" (0.1g dextran sulfate, 1 ml of 20X SSC buffer, 1 ml of formamide and 8 ml of nuclease-free water) with a dsRED2 RNA probe (Q670, LGC Biosearch Technologies, diluted 1:500) overnight at 37C. Cells were then washed with WB for 30 min, followed by 2X SSC buffer containing DAPI for 30 min. Cells were left in 2X SSC for imaging.

2.6. High throughput microscopy and image analysis

Image data sets were collected using a Yokogawa CV8000 spinning disk high throughput confocal microscope utilizing an Olympus 20x/0.75 objective and appropriate emission filters as dictated by the experimental layout. 4 field of views/well and z-stacks (1 μm optical sections) were collected, and TIFF files were maximum intensity-projected using the Yokogawa CellPathfinder software. Cell, nucleus, and PRL array segmentation, plus intensity-based feature extraction, were performed using the myImageAnalysis web application powered by Pipeline Pilot software (Biovia), as previously described [32,38]. In brief, background correction was performed using a rolling ball algorithm. Nuclear shape and intensity filters were used to filter out debris based off the DAPI signal. A nuclear mask was generated based on the DAPI channel, then used for identifying changes in nuclear GFP signal. An "array" mask was generated by identifying the area of the nucleus with the 5 % brightest GFP intensity, this mask was used to quantify GFP-ERβ array metrics. A dsRED2 array mask was generated by identifying the 5 % brightest far red (Q670) signal within the nuclear mask, used to determine the transcriptional output at the array. Aggregated, mitotic and apoptotic cells were removed using filters based on nuclear

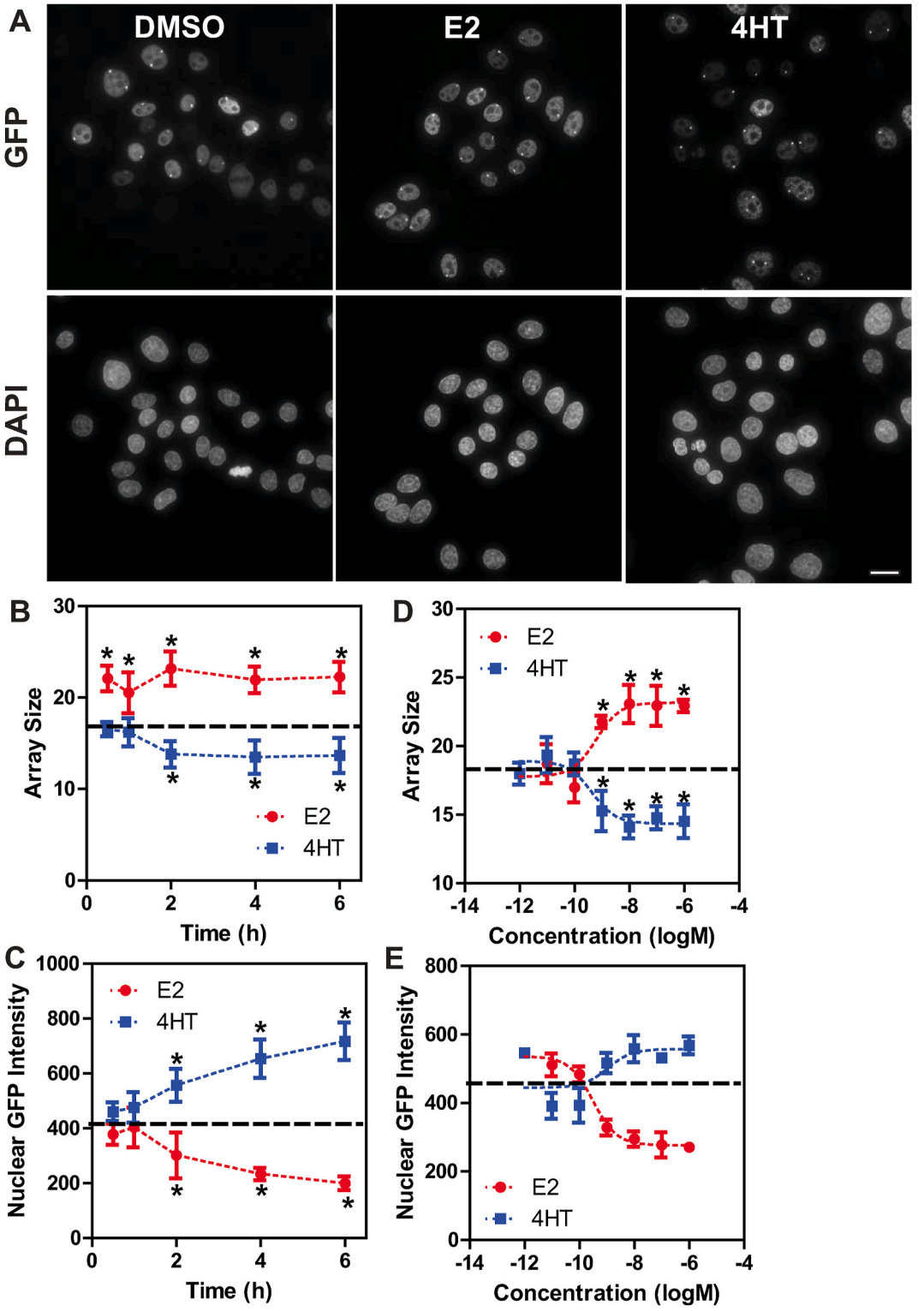

(caption on next page)

Fig. 1. Characterization of GFP-ERβ:HeLa array cells
A) Representative images of GFP-ERβ:PRL-HeLa cells taken following 2-h of the indicated treatments (DMSO, E2 100 nM, 4HT 100 nM). Images are maximum intensity projections acquired at 60x/1.42 and deconvolved. Scale bar:10 μm. B–C) array size (pixels, B) and nuclear GFP intensity (C) metrics after time course analysis of GFP-ERβ:PRL-HeLa cells treated with E2 (10 nM) and 4HT (100 nM). D-E) six-point dose response analysis at the 2-h time-point with E2 and 4HT (1pM to 1 μM) measuring array size (D) and nuclear GFP-ERβ levels (E). In panels B–E the dashed line represents the DMSO control. *$p < 0.05$ as compared to DMSO control. Error bars are from eight technical replicates.

size, nuclear shape, and nuclear intensity.

High magnification and resolution images were captured on a Cytivia DVLive deconvolution microscope using an Olympus PlanApo 60×/1.42 objective. Nuclei were captured by z-stacking with a 0.25 μm optical spacing. Images were deconvolved using SoftWorx restorative deconvolution algorithm and then maximum intensity projected.

2.7. ERE:GFP zebrafish protocols and imaging

Transgenic zebrafish were obtained and handled through the BCM Advanced Technology Zebrafish Core. Adult zebrafish were raised on a 14-h light, 10-h dark cycle in the BCM Zebrafish Research Facility on a Tecniplast recirculating water system (Tecniplast S. p.A., Buguggiate, Italy). All zebrafish used for experiments were *Tg(5xERE:GFP)c262* [36,37]. All zebrafish experiments were approved by the BCM Institutional Animal Care and Use Committee.

Adult zebrafish were allowed to spawn naturally in groups for 1 h, after which embryos were harvested. Embryos were collected in 60 cm^2 Petri dishes in E2B with methylene blue (7.5 mM NaCl, 0.25 mM KCl, 0.5 mM $MgSO_4$, 75 μM KH_2PO_4, 25 μM Na_2HPO_4, 0.5 mM $CaCl_2$, $NaHCO_3$, 0.00005 % methylene blue) before being sorted into densities of no more than 100 embryos in new 60 cm^2 Petri dishes containing E3B (5 mM NaCl, 0.17 mM KCl, 0.33 mM $CaCl_2$, 0.33 mM $MgSO_4$, 0.00002 % methylene blue), and then stored in an incubator at 28.5 °C on a 14-h light, 10-h dark cycle until treatment. Embryos (still within their chorions) were plated into a 96-well plate that was preloaded with the chemicals of interest. Using a 1000 μl pipet tip with the narrow end cut off, embryos were collected 3 at a time in 200 μl E3B for each well of the plate. Completed plates were then stored in a completely dark incubator at 28.5 °C until embryos were ready to be imaged. Embryos were allowed to hatch naturally from their chorions.

Zebrafish were anesthetized using tricaine at 25 μg/mL. Plates were then imaged (brightfield and GFP channels) using the Yokogawa CV8000 microscope using an Olympus 4x/0.16 objective scanning the whole well. A z-stack of 500 μm was collected at 50 μm steps, converted into maximum intensity projections for image analysis. Each image was qualitatively evaluated by visual inspection and scored for number of zebrafish, zebrafish that were dead or abnormal (for example, exhibiting a curved spine or other morphologic abnormalities), GFP signal in the heart valves, and GFP signal in the liver.

2.8. Statistical analysis

All statistical analyses (*t*-test and two-way ANOVA) and EC_{50} curve fitting were performed either in mIA [38] or GraphPad and significance was set at $p < 0.05$. Every experiment was repeated in 2–3 biological replicates with a minimum of four technical replicates.

3. Results

3.1. Generation and validation of an inducible GFP-ERβ:PRL-HeLa model for imaging-based high throughput screening

The paucity of contextual assays for analyzing the effects of chemicals on ERβ prompted us to generate a new model based on the previously established PRL-array system [28–33] that allows for multi-parametric analysis of ER-mediated mechanisms of transcriptional responses. Because of the constitutive and clonal nature of our previous ERβ model [29] and the identification that inducible systems granted a higher sensitivity of responses to chemicals by ERα [32], we decided to re-design the original GFP-ERβ:PRL-array model with an inducible, GFP N-terminally tagged ERβ. The full-length ERβ coding sequence was cloned in the pGFP-C1 expression vector followed by insertion into a viral vector containing the tetracycline-inducible promoter [32]. After the parental PRL-HeLa cells were transduced, cell sorting, and single cell cloning were employed to generate the final GFP-ERβ:PRL-HeLa cell line. Validation and tuning of ERβ expression were performed by Western blot, immunofluorescence, and doxycycline dose-response (Supplemental Fig. 1). This model, due to specific expression of GFP-tagged proteins, also facilitated the validation of the specificity of three commercial ERβ antibodies, when compared to ERα-containing cells. Of note, two out of three antibodies (from MilliporeSigma and GeneTex) showed specificity for ERβ with the immunofluorescence protocol performed as described in Material and Methods.

Prior to doxycycline (DOX) addition there was minimal expression of the GFP-ERβ fusion or the dsRED2 reporter mRNA (Supplemental figure 1C and fig. 2A). Optimal ERβ expression was obtained following 24h of DOX addition based on GFP signal quantification in the nucleus.

To confirm the hormonal responsiveness of the new model, cells were treated with DMSO control, the ER agonist 17β-estradiol (E2, 10 nM) or the Selective Estrogen Receptor Modulator 4-hydroxytamoxifen (4HT, 100 nM) and fixed at several time points over a 6-h period (Fig. 1B) to determine the time and differences in response to known ligands. Fig. 1A shows representative images of the GFP

channel (GFP-ERβ) at the 2-h time point, which was chosen for subsequent experiments as we aimed to develop a rapid assay for EDCs, comparable with our current ERα models, and, as expected, a bright nuclear spot (PRL array) was visible above the nucleoplasm background. From the images we noticed that a subpopulation of GFP-ERβ:PRL-HeLa contained two integrations of the regulatory cassette (PRL array) leading to two visible spots within the nucleus. We decided that, when analyzing any feature based on the PRL array, only the single brightest spot in each nucleus would be included.

Interestingly, GFP-ERβ localized to the PRL array more frequently in DMSO controls (60–80 %) versus previous ERα (between 5 and 25 %, [32]) and ERβ (~10 %), [29]) models. This is likely due to a difference between the ERs, where ERβ has been shown to display higher basal activity [25,39] via ligand-independent DNA binding. Also, the higher PRL array percentage in DMSO is in keeping with inducible vs. stable models, a phenomenon we do not currently understand [32].

As the percentage of positive arrays in the population was not changing upon ligand treatment in a reproducible manner, giving a negative Z' score, we initially focused on the dynamic range and reproducibility of the new model by two features: chromatin remodeling ("array size", Fig. 1B), measured by changes in size (pixels) of the visible GFP spot, and nuclear ERβ levels, measured by average GFP intensity within the nucleus ("nuclear GFP intensity", Fig. 1C). Compared to previous GFP-ERα:PRL-HeLa models, when treated with an agonist (E2) the overall size of the GFP spot is relatively smaller; however, the increase in size is statistically significant. The chromatin remodeling by dox-regulated GFP-ERβ is very similar to published data [29] using the previous, stable GFP-ERβ: PRL-HeLa model. Time-course analysis shows statistically significant differences between E2, 4HT, and DMSO controls in array size with E2 increasing array size and 4HT decreasing it, as expected (Fig. 1B). The overall fold change to the array size was between 1.3-1.5x compared to control, representing a smaller change to array size compared to ERα models, which can reach 2–4 fold in size after agonist exposure [32]. As previously shown for ERα, E2 addition causes ERβ turnover and subsequent decrease in nuclear ER levels, whereas 4HT addition stabilized the receptor, leading to an increase in GFP-ERβ signal within the nucleus (Fig. 1C).

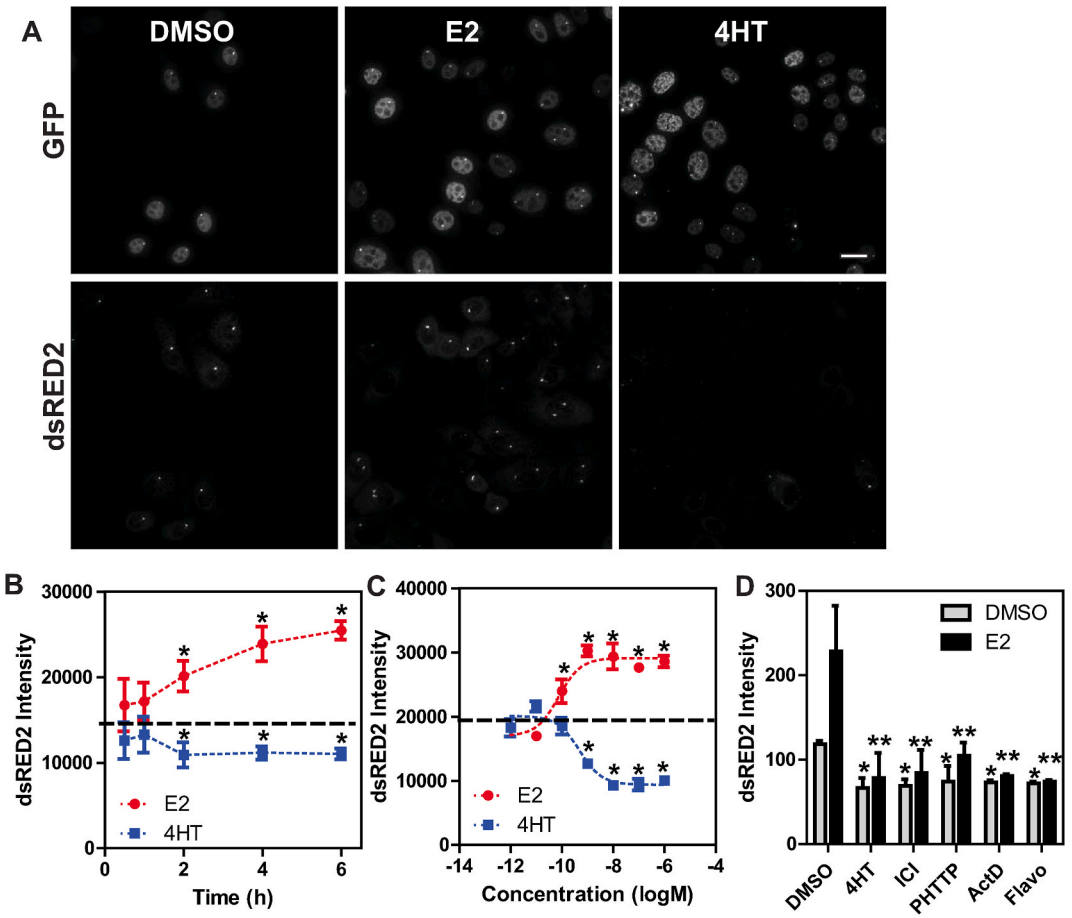

Fig. 2. ERβ elicits a strong and reproducible transcriptional response from the PRL array
(A) Representative images of dsRED2 smFISH after DMSO, E2 (10 nM), or 4HT (100 nM) treatment for 2-h; (B) quantitation of dsRED2 intensity at the PRL array after a time course treatment with E2 (10 nM) or 4HT (100 nM); C) E2 and 4HT dose-response analysis of the dsRED2 response at 2-h; and D) effect of the indicated antagonists on basal and E2 (10 nM)-stimulated dsRED2 transcription. Cells were treated with 4HT (1 μM), ICI182,780 (ICI, 1 μM), PHTTP (1 μM), actinomycin D (ActD, 1 μg/ml), and flavopiridol (Flavo, 100 nM) ± E2 10 nM *$p < 0.05$ as compared to DMSO control; **$p < 0.05$ as compared to E2 treated cells. All experiments are represented as mean and standard deviation from eight technical replicates.

To initially characterize the sensitivity of the new model, an E2 and 4HT 6-point dose response (10pM to 1 μM) was conducted at the 2-h time point (Fig. 1D–E). Through this analysis we calculated an EC_{50} value for each of the two metrics (array size: E2 62pM, 4HT 43pM; nuclear GFP: E2 31pM 4HT 1 nM).

As the PRL-array model contains a dsRED2 reporter gene linked to the ERE rich multimerized enhancers, it can also be used to quantify rapid transcriptional responses by using smFISH that targets the dsRED2 reporter gene mRNA [29,32]. Despite a basal level of transcription, likely due to ligand independent actions of ERβ at the array prior to hormone addition, the intensity of the dsRED2 RNA signal at the array increased ~3-fold in the presence of E2 while diminishing significantly when treated with 4HT (Fig. 2A–B), confirming that the basal transcriptional level observed in the DMSO samples is indeed ER-dependent. This was further established with the addition of other ER antagonists (Fig. 2D).

E2 time course analysis revealed that the transcriptional response continued to increase over the time course studied being significant as early as 1-2-h (Fig. 2B). Similarly, 4HT treatment continually decreased the transcriptional response in the same time frame.

An E2 and 4HT dose response was performed at the 2-h time point (Fig. 2C). The calculated EC_{50} for E2 and 4HT are 7.5pM and 48pM, respectively. As the dynamic range of the ERβ response is relatively small, we ran a small campaign of 384 well plates (four technical replicates and four biological replicates) to calculate assay reproducibility of the array size and nuclear GFP intensity metrics. The assay showed significant reproducibility with Z-prime scores, a canonical measure of high throughput assay quality and dynamic range, of 0.47–0.78 for calculated metrics for both agonists and antagonists (Table 1), making the new ERβ model suitable for high throughput screening of chemicals.

We then proceeded to test if known antagonists, both pan-ER and ERβ specific, would be able to reverse the transcriptional induction by E2. Cells were treated with the ER antagonists, 4HT, ICI182,780 (Fulvestrant) and PHTTP, plus the canonical transcriptional inhibitors flavopirodol and actinomycin D, as additional controls. All ERβ antagonist and transcriptional inhibitors significantly decreased both basal transcription and E2-induced stimulation of the dsRED2 mRNA (over a 2-fold decrease), as predicted (Fig. 2D).

Thus, this model is robust for screening by measuring three different mechanistic features (chromatin remodeling, protein turnover, and transcriptional output), which can be measured simultaneously, providing a powerful tool for evaluation of chemicals that affect the ERβ pathway.

3.2. *The GFP-ERβ:PRL-HeLa model responds properly to ER subtype selective agonists and antagonists*

Using the transcriptional response and chromatin remodeling features described above, we sought to confirm the ability of the GFP-ERβ:PRL-HeLa model to maintain selectivity to known ERα and ERβ selective compounds. Using the GFP-ERβ:PRL-HeLa and the previously published tet-regulated GFP-ERα:PRL-HeLa [32], we tested the ERβ selective agonists DPN and genistein, the ERβ selective antagonist PHTTP, the ERα selective agonist PPT, and the ERα antagonist MPP [3,5,40,41]. After 2-h treatments, as predicted, these test compounds behaved as agonist or antagonist, with DPN, PHTPP and genistein showing a preference for ERβ across the array metrics measured.

Fig. 3A shows a heatmap with the $logEC_{50}$ for each metric and each treatment described. The value was set to 1 for compounds where an EC_{50} could not be calculated (*e.g.*, no response). Example dose-response curves of the effects of DPN, PPT, MPP and PHTTP on dsRED2 transcriptional output across both GFP-ERα:PRL-HeLa and GFP-ERβ:PRL-HeLa are shown in Fig. 3B.

3.3. *Determination of compounds that affect ERβ using the EPA45 library, and comparison with ERα*

To obtain a baseline effect of potential EDCs on ERβ, we leveraged the EPA45 library of estrogenic compounds, that has been used by the ToxCast initiative for characterizing ERα high throughput assays and to create models of the ER pathway that can predict *in vivo* activity of environmental estrogens [23]. This small library contains ERα agonists, antagonists, and potentially inactive compounds. As a reminder, currently in ToxCast there is only one HT ERβ assay, a BiFC assays that measures dimerization of the LBD (only, without a nuclear localization signal - NLS) upon ligand binding (OT_ER_ERbERb). We performed a 6-point dose-response of the EPA45 library at the 2-h time point in three independent biological replicates with four technical replicates and calculated the EC_{50} for the array size and dsRED2 transcriptional response, as described above.

In Fig. 4A the heatmap represents the maximal fold change that a compound elicited in each feature as compared to DMSO. As compared to ERα assays [29,30,32], the magnitude of change is relatively small (dynamic range 0.27–2.37) potentially causing a larger number of false negatives. However, hierarchical clustering clearly showed a group of 15 compounds (~30 %) that altered both features >20 % reproducibly across runs, followed by a subset that changed one of the features >20 % (11 compounds), whereas the rest of the compounds had no effect. In Fig. 4B–C, we show the $logEC_{50}$ comparison between the GFP-ERβ:PRL-HeLa model and the BiFC assay from ToxCast. Overall, >50 % of the compounds had effects in at least one of the PRL array features. The previously-reported BiFC assay had 5 additional hits (methoxychlor, fenarimol, dicofol, benzylbutylphthalate and p,p'-Dichlorodiphenyldichloroethylene (p,p'DDE)) with a $logEC_{50}$ that was *higher* than the concentration we tested in our cell model. On the other

Table 1
Z-prime analysis of GFP-ERβ:PRL-HeLa image analysis extracted features.

Treatment	Array Size	dsRED2 array intensity
E2	0.60 ± 0.14	0.78 ± 0.10
4HT	0.61 ± 0.13	0.47 ± 0.1

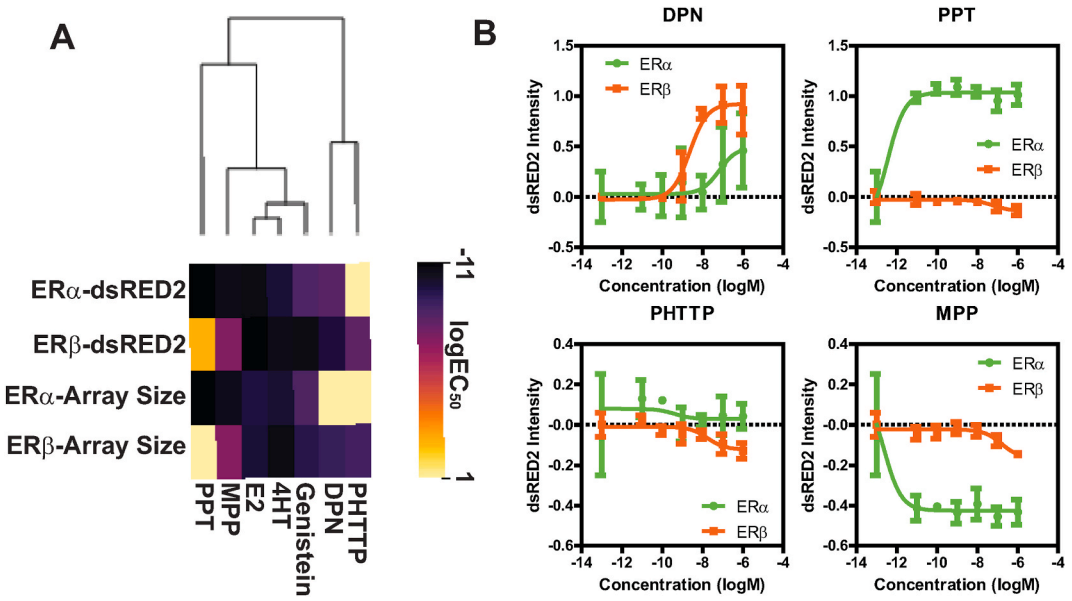

Fig. 3. Comparison of ERα/ERβ PRL-HeLa biosensor models shows model sensitivity in differentiating ER selective compounds
(A) Heatmap showing $logEC_{50}$ values for GFP-ERβ:PRL-HeLa and GFP-ERα:PRL-HeLa cells treated with the indicated chemicals (10pM to 1 μM) for 2-h as measured by transcriptional reporter and chromatin remodeling features; (B) Transcriptional response (dsRED2) of ERα (red) and ERβ (green) PRL-array cells treated with multiple doses of a ERβ selective agonist (DPN), a ERβ selective antagonist (PHTTP), a ERα selective agonist (PPT), or a ERα selective antagonist (MPP). Results are shown as mean and standard deviation from 8 technical replicates. (For interpretation of the references to colour in this figure legend, the reader is referred to the Web version of this article.)

hand, we identified five compounds that showed response in both features but no effect in the BiFC assay: kaempferol, phenobarbital, kepone, corticosterone and cycloheximide. Full dose-response curves for corticosterone and phenobarbital are shown in Fig. 4D–E. We should note here that in the batch of EPA45 chemicals we received, bisphenol A, bisphenol B, diethylstilbestrol (DES) and genistein were inactive. We tested independent batches of four out of five of these chemicals that were inactive in the EPA45 batch (DES was not available) and confirmed activity for genistein and bisphenol A, while bisphenol B showed little activation of dsRED2 which is in keeping with our original observations [29].

We then obtained a new batch of the EPA45 library from the EPA and re-performed the screen at the 2 h time point, this time comparing directly the ERβ cell line with our other inducible model expressing ERα [32]. Overall, the two receptors were comparable in terms of active compounds in the EPA45 library, please note that compounds that had no effect (no array formed or no calculatable EC_{50}) were assigned a $logEC_{50}$ of −4, a concentration higher than any that was tested. Overall, perhaps as expected, the majority of the compounds behaved very similarly between the two ERs and across both features (Fig. 5A–B). In Fig. 5, we represented the data as $logEC_{50}$ changes in array size (Fig. 5A) and dsRED2 transcriptional output (Fig. 5B) as a scatter plot highlighting "ERα preferential" vs. "ERβ preferential" chemicals when the difference in $logEC_{50}$ was >3 and was calculated for both receptors. This screen confirmed that the vast majority of EPA compounds can affect both ERs similarly, highlighting the need to develop more ERβ assays with *in vivo* relevance.

3.4. *ERE:GFP reporter transgenic zebrafish is as a rapid orthogonal assay for validating ERβ ligands in vivo*

Given the identification of few EDCs with ERα/ERβ selectivity within the EPA45 compound set, we sought to test them in an orthogonal model. As there are few *in vivo* models for ERβ, we selected a transgenic zebrafish model with an ERE-GFP reporter that was previously used as a tool for testing EDCs, that also showed the capability of comparing ERα vs ERβ responses [36,37]. The model was designed to detect estrogenic activity driven by zebrafish ERs (zERα, zERβ1, and zERβ2) on an ERE-containing reporter that produces GFP after stimulation in specific organs of the fish. The zERs show region-specific expression at 3 days post fertilization (dpf), with zERα expression localized in the heart valve and zERβ2 in the liver. It is important to note that zERα corresponds to human ERβ, with zERβ corresponding to human ERα [37]. At this stage of development zERβ1 is very low-expressed. This spatial separation of expression of the zERs (and ERE-GFP activation) provides a tool for testing EDC selectivity in an *in vivo* model at medium throughput rates using high throughput spinning disk confocal microscopy. To ensure that we were able to screen EDCs using our HT platform, we first tested the ERE:GFP zebrafish model using control compounds (E2, DPN, and genistein) at a few doses, including previously characterized EC_{50} values in the fish [36,37]. Embryos were collected and added to 96 well plates pre-loaded with the test compounds. At 3 days post fertilization (dpf) the embryos were anesthetized and imaged (Fig. 6A–D, Table 2). E2 induced GFP signal in both the heart valve and liver at concentrations as low as 10 nM (Fig. 6B), reproducing previously published results (EC_{50} ~3–5 nM, [36,37]). DPN and genistein both showed heart valve and liver signal at 10 μM (Table 2) and only heart valve signal at 1 μM (Fig. 6C–D)

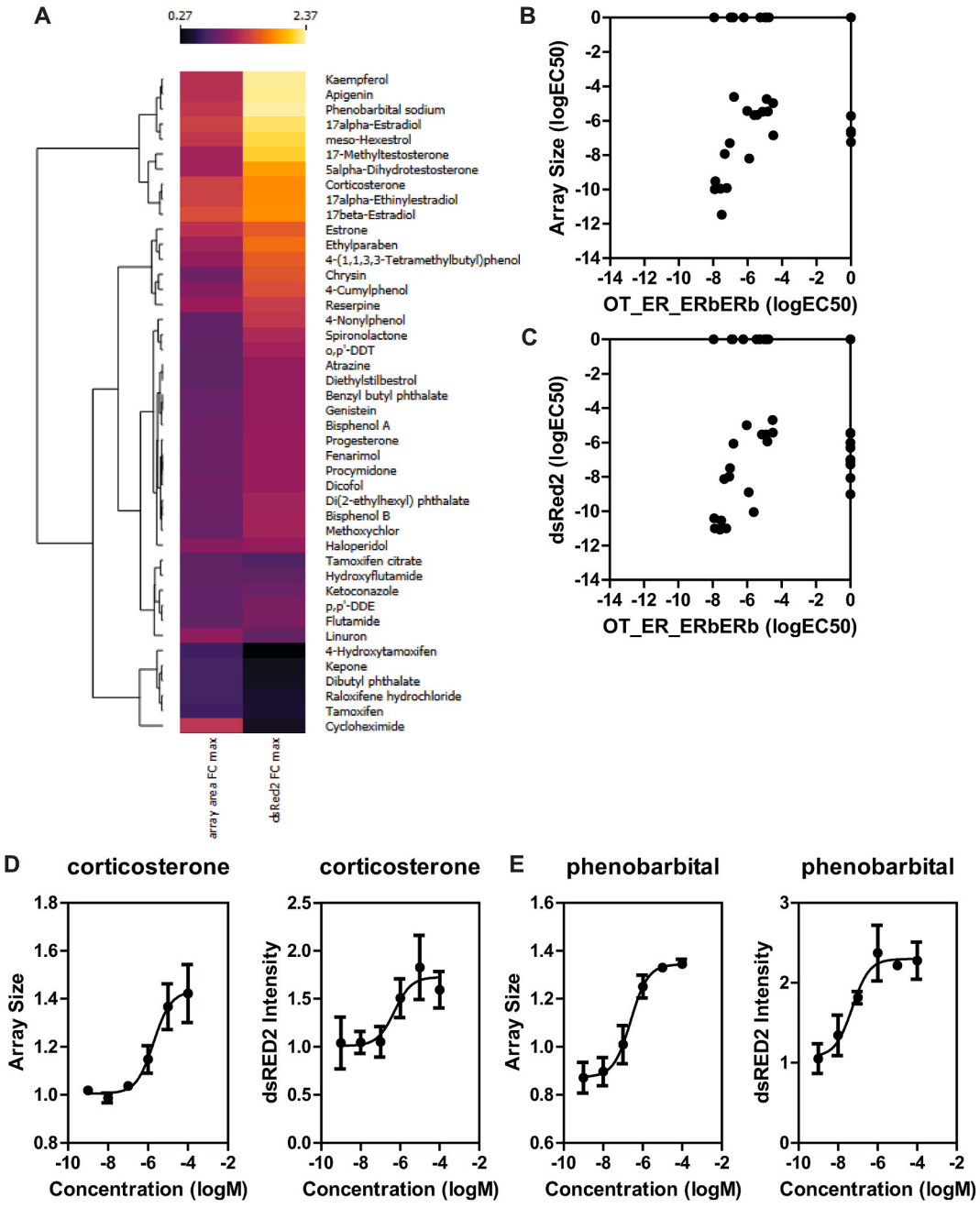

Fig. 4. EPA45 Compound library comparison to ToxCast ERβ dimerization data
A) Heatmap showing the effect of EPA45 chemicals on the GFP-ERβ:PRL-HeLa cell line represented as maximal fold change over DMSO control. Data is shown as average of three independent screens. B–C) Comparison of determined $logEC_{50}$ values of GFP-ERβ:PRL-HeLa array size (B) and dsRED2 intensity (C) vs. Odyssey Thera BiFC ERβ-ERβ dimerization assay. D-E) dose-response analysis for corticosterone (D) and phenobarbital (E) using the array size and dsRed2 intensity metrics. Data is average ± standard deviation of three independent experiments.

confirming the predicted selectivity for zERα (hERβ). These results faithfully reproduced previously published ERα and ERβ data [36,37]. As previously reported for the ERE-GFP zebrafish model, the zebrafish reporter model and GFP-ER:PRL-HeLa models reveal a ~2 log sensitivity decrease in the zebrafish model as the concentration in the water does not correspond to the concentration of chemical up taken by the fish [37,45].

We then used the ERE:GFP Zebrafish reporter as an orthogonal model to confirm if the five novel chemicals identified as ERβ ligands as compared to ToxCast data (Fig. 4) could also work *in vivo*. Each compound was tested at 2 concentrations (2 and 20 μM) which were pre-spotted on the treatment plate (Table 3). Embryos were added and imaged at 3 dpf. Of the 5 novel compounds tested, two

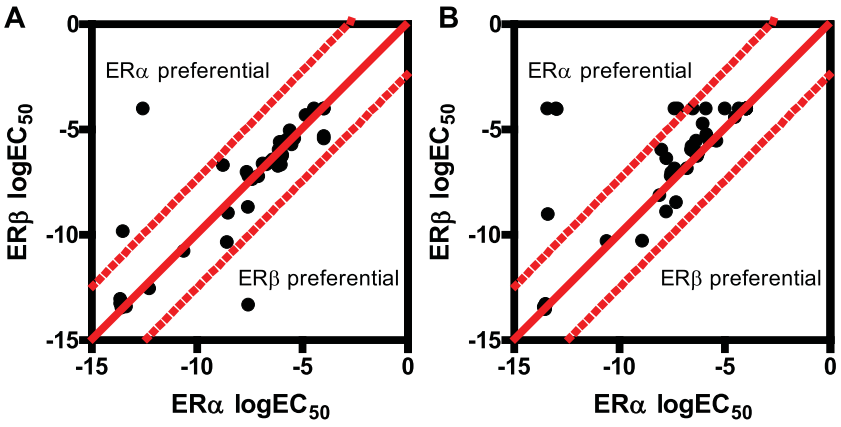

Fig. 5. Comparison of ERs using PRL-HeLa models identifies ERβ interacting compounds in the EPA45 library of control chemicals
Scatter plots comparing $logEC_{50}$ values for the array size (A) or the dsRED2 transcriptional output (B) metrics in ERα and ERβ-containing cells treated for 2-h with a six-point dose-response of the EPA45 chemical library.

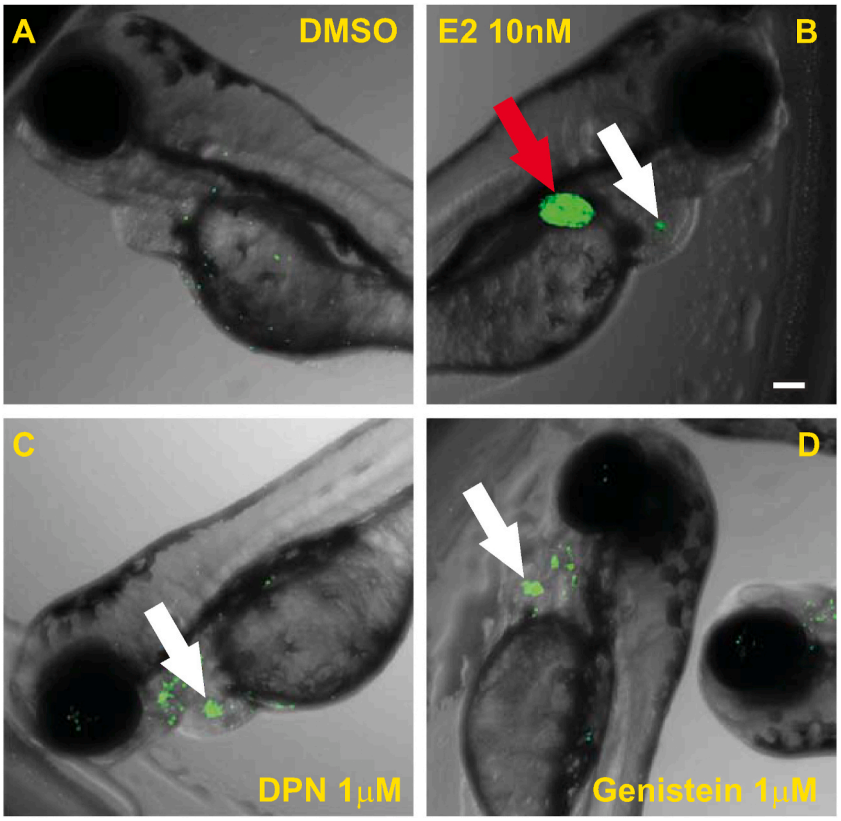

Fig. 6. Transgenic ERE:GFP reporter zebrafish as an *in vivo* orthogonal assay to define ERα vs. ERβ activities
Representative images of the ERE:GFP Zebrafish at 3dfp treated with: (A) DMSO; (B); 10 nM E2; (C) 1 μM DPN; and, D) 1 μM genistein. Red arrows highlight GFP signal in the liver while white arrows indicate the heart valve. Whole-well images were captured at 4x/0.16. Scale bar is 100 μm. A minimum of ten Zebrafish per treatment were assayed. (For interpretation of the references to colour in this figure legend, the reader is referred to the Web version of this article.)

showed GFP signal in both the liver and heart valve at both concentrations tested, corticosterone and phenobarbital sodium, in keeping with other results for ERα [29,30,32]. The remaining three compounds showed no activity in either the heart valve or liver, with cycloheximide being mostly toxic, confirming its status as a likely false positive due to assay interference due to inhibition of protein synthesis. The low rate of validated hits is not unexpected. As noted previously, the sensitivity of the zebrafish model is significantly

Table 2
qualitative analysis of ERE:GFP reporter zebrafish treated with three doses of control chemicals.

Compound	Concentration	Liver		Heart Valve		Toxicity	
E2	100 nM	12	/12	12	/12	0	/12
	10 nM	10	/11	10	/11	0	/11
	1 nM	0	/12	0	/12	0	/12
DMSO	1:10	0	/11	0	/11	0	/11
	1:100	0	/12	0	/12	0	/12
	1:1000	0	/12	0	/12	1	/12
DPN	100 μM	10	/12	11	/12	0	/12
	10 μM	12	/12	12	/12	0	/12
	1 μM	0	/12	12	/12	0	/12
genistein	100 μM	6	/12	6	/12	12	/12
	10 μM	12	/12	12	/12	0	/12
	1 μM	0	/11	11	/11	0	/11

lower than that of the PRL-HeLa models. Additionally, many of the compounds tested were weak positives ($\log EC_{50} < -7$) and thus may not be active in the fish except at unachievably high levels (*e.g.*, DMSO concentration would be too high in the water causing toxicity).

Overall, the ERE:GFP zebrafish model confirmed potentially novel ERβ ligands that were identified with the GFP-ERβ:PRL-HeLa model, including a few previously characterized as inactive by the ToxCast BiFC assay.

4. Discussion

The industrial era opened the door for thousands of man-made chemicals to enter the environment and thus directly impact wildlife and human health. A growing number of these chemicals with varying structures, termed endocrine disrupting chemicals (EDCs), have been shown to interfere with many aspects of human physiology, from development to reproductive biology [1,12,16,18]. The most common target for EDCs is the estrogen receptor (ER), a master transcriptional regulator, which is responsible for female reproduction among many other roles [1]. There are two ER proteins, transcribed from different genes, ERα and ERβ, which share a common mechanism of action. While being structurally similar, they differ greatly in terms of their biological roles, with ERα usually considered a pro-proliferative, anti-apoptotic transcription factor, and ERβ being a tumor suppressor. Despite a very close similarity in their ligand binding domains, subtle amino acid differences and the size of the ligand binding pocket allow for chemicals to bind to both receptors or preferentially to one, which also opened the door for their use for therapeutical purposes [3,4,9,11].

In the vast realm of EDCs, phytoestrogens have been shown to interact with both receptors, even though many prefer ERβ (*i.e.*, genistein, liquiritigenin, daidzein etc.); the same applies to bisphenol A analogs, some of which we and others identified as potential ERβ antagonists [6,26,27,29,42,43]. Because of the growing number of chemicals and their mixtures, there is a continuous need to develop fast, sensitive, and contextual high throughput assays for detection and mechanistic evaluation. In response to this need we have previously developed and implemented several engineered ER, PR, and AR HeLa cell models for robust high throughput screening and high content analysis [28–32,34,35]. These models leverage doxycycline inducible GFP-tagged ER (or the other chimeric receptors) and a multicopy ERE-rich super enhancer derived from the prolactin (PRL) gene, linked to a transcriptional reporter (dsRED2). When bound by GFP-ER fusions, the dense focal integration of EREs results in the formation of a visible nuclear spot detectable by fluorescent microscopy referred to as a chromatin "array." This HT high content assay approach enables single cell-based quantitative analysis of accumulated transcriptional reporter mRNA along with several phenotypic features from the array (*i.e.*, size) that report on mechanistic metrics of the ER pathway including nuclear accumulation and large-scale chromatin remodeling.

Over the years, dozens of high throughput assay were developed focusing mostly on ERα, including those used by the ToxCast and Tox21 initiatives that ultimately lead to an 18 *in vitro* assay panel capable of predicting the *in vivo* effects of chemicals tested cell culture models [21–24]. Interestingly, ERβ has been largely ignored in these large initiatives, with only a single high-throughput ERβ assay, a BiFC assay being included in ToxCast using the ERβ LBD tagged with a fluorescent protein to measure receptor dimerization. Part of the

Table 3
ERβ ligands identified uniquely in the PRL-array system tested in the ERE:GFP Zebrafish model.

Compound	Stock	Heart (zERα/hERβ)	Liver (zERβ/hERα)	Dead/Abnormal
Corticosterone	20 μM	16/18	16/18	2/18
	2 μM	18/18	18/18	0/18
Cycloheximide	20 μM	1/18	1/18	8/18
	2 μM	0/18	0/18	0/18
Kaempferol	20 μM	1/18	0/18	0/18
	2 μM	0/18	0/18	0/18
Kepone	20 μM	0/18	0/18	0/18
	2 μM	0/18	0/18	0/18
Phenobarbital sodium	20 μM	14/18	16/18	1/18
	2 μM	17/18	16/18	1/18

problem is that ERβ biology has been overall less studied. However, experimental hindrances have also been a major issue including lack of quality reagents, such as ERβ selective antibodies, and lack of *in vitro* cell lines that maintain ERβ expression over time; limiting the possibilities of developing assays with endogenous ERβ.

In this study we validated a novel ERβ biosensor model capable of rapidly and accurately identifying EDCs that impact ERβ activity, including selectivity over ERα. One of the major benefits of the inducible GFP-ERβ:PRL-HeLa assay is the ability to measure multiple mechanistic features of the ER signaling pathway in parallel, greatly expanding our ability to understand ligand effects on ERβ, namely nuclear levels of GFP-ERβ, chromatin remodeling ("array size") and transcriptional readout (dsRED2 intensity). In addition to enhancing the number of fast and reproducible assays and the ability to detect novel ERβ EDCs, the GFP-ERβ:PRL-HeLa serves as a tool for comparing activity of any given compound between the two ERs. By comparing the GFP-ERβ:PRL-HeLa to previously published GFP-ERα:PRL-HeLa model [32] we were able to demonstrate the selectivity of several known selective modulators of the ERs, including genistein, DPN, PPT, and PHTTP.

Testing of the EPA45 reference compound set demonstrated an increased assay sensitivity and an ability to identify ERβ EDCs that were previously missed in earlier screens using this small library. In part, additional 'hit' calling is due to the increased sensitivity of the assay combined with measuring multiple features. As with any HT assay, a portion of the hits will be due to assay interference and not be directly linked to the pathway studied (*i.e.*, toxic and non-specific compound). One example in our study is cycloheximide, a known protein translation inhibitor that was considered a hit through its effects on transcriptional output and chromatin remodeling, but through a completely different and well-established mechanism of action (global inhibition of protein synthesis). We faced the same issue in a recent study looking at endogenous ER levels [44], which emphasizes the need for orthogonal assays for hit validation. For ERβ, a potential orthogonal assay is through the use of transgenic zebrafish engineered with an ERE-GFP reporter that reports on estrogenic activity in different tissues, combining mechanistic readout with an *in vivo* complex organism [36,37].

By utilizing the spatial separation of zERs (heart valve for ERβ and liver for ERα) at 3 dpf, the model is well suited to evaluate compound activity on both ER subtypes in a high throughput/high content assay manner. We utilized this system with a set of known chemicals and hits from the GFP-ERβ:PRL-HeLa assay and were able to confirm the activity of two novel hits (corticosterone and phenobarbital sodium). This is incredibly exciting as it demonstrates that compounds identified by the GFP-ERβ:PRL-HeLa assay are not only accurate but are also active in an organismal model system and may have relevance in environmental contexts and.

In conclusion, we generated and validated a novel ERβ-centric, mechanistically relevant high throughput assay whose results hold true in a transgenic *in vivo* zebrafish model, collectively adding a novel assay to the current list of available ones for use in environmental testing and drug development. The addition of this powerful ERβ model fills a much-needed role in screening chemical libraries and environmental samples for ERβ selective compound identification. Furthermore, as the ability to selectively modulate ER is a key therapeutic option in multiple disease and cancer types, our complementary cell culture (ERα/ERβ) and zebrafish models should be useful to aid in the identification of selective ER ligands to supplement the therapeutic toolbox.

DATA AVAILABILITY statement

The data associated with this study has not been deposited into a publicly available repository but will be made available on request.

Funding statement

Imaging for this project was supported by the Integrated Microscopy Core at Baylor College of Medicine and the Center for Advanced Microscopy and Image Informatics (CAMII) with funding from NIH (DK56338, CA125123, ES027704, ES030285, S10OD030414), and CPRIT (RP170719).

CRediT authorship contribution statement

Derek A. Abbott: Writing - review & editing, Writing - original draft, Visualization, Validation, Methodology, Investigation, Formal analysis, Data curation, Conceptualization. **Maureen G. Mancini:** Resources, Methodology, Investigation, Data curation. **Michael J. Bolt:** Visualization, Validation, Methodology, Investigation, Formal analysis, Data curation. **Adam T. Szafran:** Software, Methodology, Formal analysis, Data curation. **Kaley A. Neugebauer:** Resources, Methodology. **Fabio Stossi:** Writing - review & editing, Writing - original draft, Visualization, Validation, Supervision, Methodology, Investigation, Formal analysis, Data curation, Conceptualization. **Daniel A. Gorelick:** Resources, Methodology. **Michael A. Mancini:** Writing - review & editing, Writing - original draft, Supervision, Resources, Project administration, Funding acquisition, Conceptualization.

Declaration of competing interest

The authors declare that they have no known competing financial interests or personal relationships that could have appeared to influence the work reported in this paper.

Appendix A. Supplementary data

Supplementary data to this article can be found online at https://doi.org/10.1016/j.heliyon.2023.e23119.

References

[1] M. Jia, K. Dahlman-Wright, J.Å. Gustafsson, Estrogen receptor alpha and beta in health and disease, Best Pract Res Clin Endocrinol Metab 29 (4) (2015) 557–568.
[2] R.P.A. Barros, J.Å. Gustafsson, Estrogen receptors and the metabolic network, Cell Metab 14 (3) (2011) 289–299.
[3] I. Paterni, C. Granchi, J.A. Katzenellenbogen, F. Minutolo, Estrogen receptors alpha (ERα) and beta (ERβ): subtype-selective ligands and clinical potential, Steroids 90 (2014) 13–29.
[4] F. Minutolo, M. Macchia, B.S. Katzenellenbogen, J.A. Katzenellenbogen, Estrogen receptor β ligands: recent advances and biomedical applications, Med. Res. Rev. 31 (3) (2011) 364–442.
[5] B.S. Katzenellenbogen, I. Choi, R. Delage-Mourroux, T.R. Ediger, P.G. Martini, M. Montano, et al., Molecular mechanisms of estrogen action: selective ligands and receptor pharmacology, J. Steroid Biochem. Mol. Biol. 74 (5) (2000) 279–285.
[6] G.G. Kuiper, B. Carlsson, K. Grandien, E. Enmark, J. Häggblad, S. Nilsson, et al., Comparison of the ligand binding specificity and transcript tissue distribution of estrogen receptors alpha and beta, Endocrinology 138 (3) (1997) 863–870.
[7] C. Zhao, K. Dahlman-Wright, J.Å. Gustafsson, Estrogen signaling via estrogen receptor {beta, J. Biol. Chem. 285 (51) (2010) 39575–39579.
[8] S. Nilsson, J.A. Gustafsson, Biological role of estrogen and estrogen receptors, Crit. Rev. Biochem. Mol. Biol. 37 (1) (2002) 1–28.
[9] P. Ascenzi, A. Bocedi, M. Marino, Structure-function relationship of estrogen receptor alpha and beta: impact on human health, Mol Aspects Med 27 (4) (2006) 299–402.
[10] E. Enmark, M. Pelto-Huikko, K. Grandien, S. Lagercrantz, J. Lagercrantz, G. Fried, et al., Human estrogen receptor beta-gene structure, chromosomal localization, and expression pattern, J. Clin. Endocrinol. Metab. 82 (12) (1997) 4258–4265.
[11] S.Y. Dai, T.P. Burris, J.A. Dodge, C. Montrose-Rafizadeh, Y. Wang, B.D. Pascal, et al., Unique ligand binding patterns between estrogen receptor alpha and beta revealed by hydrogen-deuterium exchange, Biochemistry 48 (40) (2009) 9668–9676.
[12] S. Amir, S.T.A. Shah, C. Mamoulakis, A.O. Docea, O.I. Kalantzi, A. Zachariou, et al., Endocrine disruptors acting on estrogen and androgen pathways cause reproductive disorders through multiple mechanisms: a review, Int J Environ Res Public Health 18 (4) (2021) 1464.
[13] E.K. Shanle, W. Xu, Endocrine disrupting chemicals targeting estrogen receptor signaling: identification and mechanisms of action, Chem. Res. Toxicol. 24 (1) (2011) 6–19.
[14] A.C. Gore, Neuroendocrine targets of endocrine disruptors, Horm Athens Greece 9 (1) (2010) 16–27.
[15] R. McKinlay, J.A. Plant, J.N.B. Bell, N. Voulvoulis, Endocrine disrupting pesticides: implications for risk assessment, Environ. Int. 34 (2) (2008 Feb) 168–183.
[16] R.T. Zoeller, T.R. Brown, L.L. Doan, A.C. Gore, N.E. Skakkebaek, A.M. Soto, et al., Endocrine-disrupting chemicals and public health protection: a statement of principles from the Endocrine Society, Endocrinology 153 (9) (2012) 4097–4110.
[17] S.H. Safe, Polychlorinated biphenyls (PCBs): environmental impact, biochemical and toxic responses, and implications for risk assessment, Crit. Rev. Toxicol. 24 (2) (1994) 87–149.
[18] M.L.Y. Wan, V.A. Co, H. El-Nezami, Endocrine disrupting chemicals and breast cancer: a systematic review of epidemiological studies, Crit. Rev. Food Sci. Nutr. 62 (24) (2022) 6549–6576.
[19] A. Lacouture, C. Lafront, C. Peillex, M. Pelletier, É. Audet-Walsh, Impacts of endocrine-disrupting chemicals on prostate function and cancer, Environ. Res. 204 (Pt B) (2022), 112085.
[20] D. Lopez-Rodriguez, D. Franssen, S. Heger, A.S. Parent, Endocrine-disrupting chemicals and their effects on puberty, Best Pract Res Clin Endocrinol Metab 35 (5) (2021), 101579.
[21] R. Judson, K. Houck, M. Martin, T. Knudsen, R.S. Thomas, N. Sipes, et al., In vitro and modelling approaches to risk assessment from the U.S. Environmental Protection Agency ToxCast programme, Basic Clin. Pharmacol. Toxicol. 115 (1) (2014) 69–76.
[22] A.M. Richard, R. Huang, S. Waidyanatha, P. Shinn, B.J. Collins, I. Thillainadarajah, et al., The Tox21 10K compound library: collaborative chemistry advancing toxicology, Chem. Res. Toxicol. 34 (2) (2021) 189–216.
[23] R.S. Judson, F.M. Magpantay, V. Chickarmane, C. Haskell, N. Tania, J. Taylor, et al., Integrated model of chemical perturbations of a biological pathway using 18 in vitro high-throughput screening assays for the estrogen receptor, Toxicol Sci Off J Soc Toxicol 148 (1) (2015) 137–154.
[24] R.S. Judson, K.A. Houck, E.D. Watt, R.S. Thomas, On selecting a minimal set of in vitro assays to reliably determine estrogen agonist activity, Regul Toxicol Pharmacol RTP 91 (2017) 39–49.
[25] W.R. Harrington, S. Sheng, D.H. Barnett, L.N. Petz, J.A. Katzenellenbogen, B.S. Katzenellenbogen, Activities of estrogen receptor alpha- and beta-selective ligands at diverse estrogen responsive gene sites mediating transactivation or transrepression, Mol. Cell. Endocrinol. 206 (1–2) (2003) 13–22.
[26] P. Gong, Z. Madak-Erdogan, J. Li, J. Cheng, C.M. Greenlief, W. Helferich, et al., Transcriptomic analysis identifies gene networks regulated by estrogen receptor α (ERα) and ERβ that control distinct effects of different botanical estrogens, Nucl. Recept. Signal. 12 (2014), e001.
[27] Y. Jiang, P. Gong, Z. Madak-Erdogan, T. Martin, M. Jeyakumar, K. Carlson, et al., Mechanisms enforcing the estrogen receptor β selectivity of botanical estrogens, FASEB J Off Publ Fed Am Soc Exp Biol 27 (11) (2013) 4406–4418.
[28] F.J. Ashcroft, J.Y. Newberg, E.D. Jones, I. Mikic, M.A. Mancini, High content imaging-based assay to classify estrogen receptor-α ligands based on defined mechanistic outcomes, Gene 477 (1–2) (2011) 42–52.
[29] F. Stossi, M.J. Bolt, F.J. Ashcroft, J.E. Lamerdin, J.S. Melnick, R.T. Powell, et al., Defining estrogenic mechanisms of bisphenol A analogs through high throughput microscopy-based contextual assays, Chem Biol 21 (6) (2014) 743–753.
[30] M.J. Bolt, P. Singh, C.E. Obkirchner, R.T. Powell, M.G. Mancini, A.T. Szafran, et al., Endocrine disrupting chemicals differentially alter intranuclear dynamics and transcriptional activation of estrogen receptor-α, iScience 24 (11) (2021), 103227.
[31] Z.D. Sharp, M.G. Mancini, C.A. Hinojos, F. Dai, V. Berno, A.T. Szafran, et al., Estrogen-receptor-alpha exchange and chromatin dynamics are ligand- and domain-dependent, J. Cell Sci. 119 (Pt 19) (2006) 4101–4116.
[32] A.T. Szafran, M.G. Mancini, F. Stossi, M.A. Mancini, Sensitive image-based chromatin binding assays using inducible ERα to rapidly characterize estrogenic chemicals and mixtures, iScience 25 (10) (2022), 105200.
[33] A.T. Szafran, F. Stossi, M.G. Mancini, C.L. Walker, M.A. Mancini, Characterizing properties of non-estrogenic substituted bisphenol analogs using high throughput microscopy and image analysis, PLoS One 12 (7) (2017), e0180141.
[34] A.T. Szafran, M.J. Bolt, C.E. Obkirchner, M.G. Mancini, C. Helsen, F. Claessens, et al., A mechanistic high-content analysis assay using a chimeric androgen receptor that rapidly characterizes androgenic chemicals, SLAS Discov Adv Life Sci R D 25 (7) (2020) 695–708.
[35] L.S. Treviño, M.J. Bolt, S.L. Grimm, D.P. Edwards, M.A. Mancini, N.L. Weigel, Differential regulation of Progesterone receptor-mediated transcription by CDK2 and DNA-PK, Mol Endocrinol Baltim Md 30 (2) (2016) 158–172.
[36] D.A. Gorelick, M.E. Halpern, Visualization of estrogen receptor transcriptional activation in zebrafish, Endocrinology 152 (7) (2011) 2690–2703.
[37] D.A. Gorelick, L.R. Iwanowicz, A.L. Hung, V.S. Blazer, M.E. Halpern, Transgenic zebrafish reveal tissue-specific differences in estrogen signaling in response to environmental water samples, Environ. Health Perspect. 122 (4) (2014) 356–362.
[38] A.T. Szafran, M.A. Mancini, The myImageAnalysis project: a web-based application for high-content screening, Assay Drug Dev. Technol. 12 (1) (2014) 87–99.
[39] P. Webb, C. Valentine, P. Nguyen, R.H. Price, A. Marimuthu, B.L. West, et al., ERbeta binds N-CoR in the presence of estrogens via an LXXLL-like motif in the N-CoR C-terminus, Nucl. Recept. 1 (1) (2003) 4.
[40] J. Sun, J. Baudry, J.A. Katzenellenbogen, B.S. Katzenellenbogen, Molecular basis for the subtype discrimination of the estrogen receptor-beta-selective ligand, diarylpropionitrile, Mol Endocrinol Baltim Md 17 (2) (2003) 247–258.
[41] H.B. Zhou, K.E. Carlson, F. Stossi, B.S. Katzenellenbogen, J.A. Katzenellenbogen, Analogs of methyl-piperidinopyrazole (MPP): antiestrogens with estrogen receptor alpha selective activity, Bioorg Med Chem Lett 19 (1) (2009) 108–110.
[42] G.G. Kuiper, J.G. Lemmen, B. Carlsson, J.C. Corton, S.H. Safe, P.T. van der Saag, et al., Interaction of estrogenic chemicals and phytoestrogens with estrogen receptor beta, Endocrinology 139 (10) (1998) 4252–4263.

[43] T.H. Charn, E.T.B. Liu, E.C. Chang, Y.K. Lee, J.A. Katzenellenbogen, B.S. Katzenellenbogen, Genome-wide dynamics of chromatin binding of estrogen receptors alpha and beta: mutual restriction and competitive site selection, Mol Endocrinol Baltim Md 24 (1) (2010) 47–59.
[44] F. Stossi, P.K. Singh, R.M. Mistry, H.L. Johnson, R.D. Dandekar, M.G. Mancini, et al., Quality control for single cell imaging analytics using endocrine disruptor-induced changes in estrogen receptor expression, Environ. Health Perspect. 130 (2) (2022), 27008.
[45] J.P. Souder, D.A. Gorelick, Quantification of estradiol uptake in zebrafish embryos and larvae, Toxicol. Sci. 158 (2) (2017) 465–474.